

# Branched Micelles by Living Crystallization-Driven Block Copolymer Self-Assembly under Kinetic Control

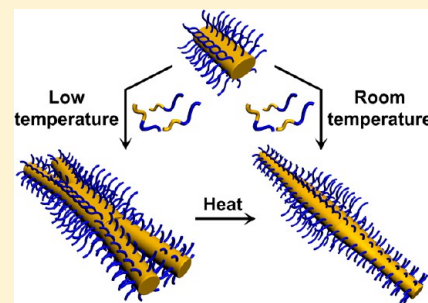
Huibin Qiu,<sup>†</sup> Yang Gao,<sup>†</sup> Van An Du,<sup>†</sup> Rob Harniman,<sup>†</sup> Mitchell A. Winnik,<sup>\*,‡</sup> and Ian Manners<sup>\*,†</sup>

<sup>†</sup>School of Chemistry, University of Bristol, Bristol BS8 1TS, United Kingdom

<sup>‡</sup>Department of Chemistry, University of Toronto, Toronto, Ontario M5S 3H6, Canada

**S** Supporting Information

**ABSTRACT:** We have found that the width and shape (from rectangular to elliptical, to almost circular in cross-section) of the crystalline core of fiberlike micelles of polyferrocenyldimethylsilane (PFDMS) diblock copolymers can be varied by altering the degree of polymerization of PFDMS, and also the chemistry of the complementary corona-forming block. This enabled detailed studies of living crystallization-driven self-assembly (CDSA) processes that involved the addition of unimers with a short, crystallizable core-forming PFDMS block to a seed solution of short micelles with a large diameter crystalline core, derived from block copolymers with a longer PFDMS block. The morphology of resultant micelles was found to be highly dependent on the polarity of the solvent and temperature. For example, linear micelles were formed in less polar solvents (which are moderately poor solvents for PFDMS) and/or at higher temperatures. In contrast, the formation of branched structures could be “switched on” when the opposite conditions were used. Thus, the use of more polar solvents (which are very poor solvents for PFDMS) and ambient or subambient temperatures allowed the formation of branched micelles and block comicelles with variable and spatially distinct corona chemistries, including amphiphilic nanostructures. Rapid crystallization of added unimers at the seed micelle termini under nonequilibrium self-assembly conditions appears to facilitate the formation of the branched micellar structures as a kinetically trapped morphology. This is evidenced by the transformation of the branched micelles into linear micelles on heating at elevated temperatures.



## INTRODUCTION

Branched structures are ubiquitous in biological systems where they enable numerous vital and complex functions. In addition, the recent preparation of branched nanoparticles, such as multipod nanocrystals,<sup>1</sup> hyperbranched<sup>2</sup> and treelike nanostructures,<sup>3</sup> and their hierarchical self-assembly into colloidal superlattices<sup>4</sup> illustrate pathways to promising new optical and electronic materials through advanced morphology control. In contrast, despite observations of branched micelle structures in self-assembled soft-matter-derived surfactant systems of both low and high molar mass,<sup>5,6</sup> these morphologies occupy a very restricted window in terms of phase space and self-assembly conditions, and no significant control over the degree of branching and junction location has been reported.

Over the past few decades, the self-assembly of block copolymers has received considerable attention due to the formation of a wide variety of morphologies either in bulk or in solution.<sup>7,8</sup> It is well-known that, when dissolved in a block selective solvent, block copolymers self-assemble to form micellar aggregates with a range of interesting applications.<sup>8</sup> The morphologies of these micelles can be controlled thermodynamically by a variety of parameters, including chain stretching of the core-forming block, intercoronal chain repulsions, and the interfacial free energy between the solvent and the micellar core. This has enabled the preparation of a diverse array of micellar morphologies such as spheres, fibers,

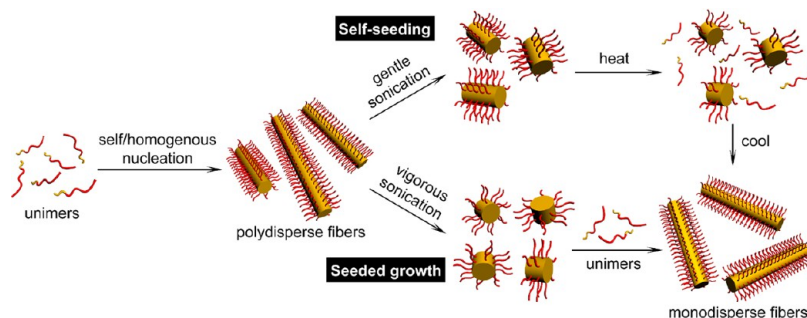
and vesicles.<sup>8</sup> In addition, kinetic manipulation techniques have enriched the morphology pool of block copolymer self-assemblies.<sup>9</sup> Compared to low molecular weight amphiphiles, block copolymers show much slower dynamics in selective solvents and the exchange of chains between micelles is generally inhibited.<sup>9,10</sup> Hence, metastable aggregates are frequently observed that are resistant to morphological transformation to thermodynamically more stable forms. This has resulted in the observation of a wide range of kinetically trapped morphologies, such as branched micelles,<sup>6</sup> multi-compartment micelles and hierarchical superstructures,<sup>11,12</sup> helical nanostructures,<sup>13</sup> and toroidal micelles.<sup>14</sup> To date, the overwhelming majority of these studies involve a core-forming block that does not crystallize and resulting micelle cores are amorphous. Although remarkable morphological diversity has been demonstrated, the ability to predict micelle shape (especially for nonspherical structures) and to control dimensions is generally limited.

Crystallization-driven self-assembly (CDSA) of amphiphilic block copolymers with a crystalline core-forming block has recently emerged as a promising and versatile complementary method with which to generate one- and two-dimensional structures.<sup>15,16</sup> In particular, CDSA can often be used as a

Received: December 13, 2014

Published: January 13, 2015

Scheme 1. Schematic Representation of Two Living CDSA Routes: (Bottom) Seeded Growth and (Top) Self-Seeding

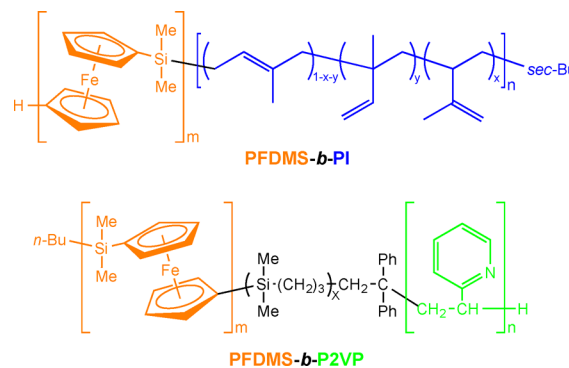


“living” process analogous to living covalent polymerizations of molecular monomers, allowing access to micelles of predictable shape that are both complex and well-defined.<sup>16g,i,q,17</sup> Living CDSA can be accomplished through two different routes (Scheme 1), namely, seeded growth<sup>17a,b</sup> and self-seeding.<sup>17c,d</sup> Seeded growth usually involves vigorous sonication of preformed polydisperse fiberlike micelles to produce very short micelle seeds and the subsequent addition of further unimers to enable elongation through epitaxial growth at the seed termini. On the other hand, in a self-seeding process, free unimers are released from micelles by a partial dissolution process involving regions of lower core crystallinity through either thermal annealing, or addition of a small amount of a good solvent for both the core- and corona-forming blocks. The remaining micelle fragments subsequently function as seeds for epitaxial growth of released unimer on cooling or removal of the good solvent. While self-seeding is generally used to improve the monodispersity of fiberlike micelles or to create micelle seeds from block copolymers that are sensitive to sonication, seeded growth can be widely applied to generate a rich variety of micellar structures.<sup>16–20</sup> For example, living CDSA has allowed access to fiberlike micelles with narrow length distribution and block comicelles with spatially distinct coronal or core chemistries, as well as micelles with a variety of complex two-dimensional shapes.<sup>16–20</sup>

In this paper, as a follow-up to our preliminary communication,<sup>21</sup> we report full details of our attempts to form branched micelle structures using living CDSA. The approach that we have explored involves two steps. First, we targeted the preparation of seed micelles with a crystalline core of large diameter from poly(ferrocenyldimethylsilane) (PFDMS) block copolymers with a long crystallizable PFDMS core-forming block. In a second step, we then investigated the addition of unimers of block copolymers with a shorter crystallizable PFDMS core-forming block to the large diameter micelles as seeds under a variety of conditions. The materials utilized in our initial studies were the diblock copolymers PFDMS-*b*-PI (PI = polyisoprene) and PFDMS-*b*-P2VP (P2VP = poly(2-vinylpyridine)), which contain hydrophobic and hydrophilic complementary blocks, respectively (Chart 1).

## RESULTS

**1. Variations in Core Dimensions and Cross-Sectional Shape of Fiberlike Micelles via Changes to the Length of the PFDMS Core-Forming Block.** (a). *PFDMS-*b*-PI Block Copolymers.* Although living CDSA has provided a method to access fiberlike micelles of controlled length and narrow length distributions, methods to control micelle width have not been

Chart 1. Structures of PFDMS-*b*-PI and PFDMS-*b*-P2VP Diblock Copolymers

reported. In principle, variation of the length of the core-forming block should allow this parameter to be varied.<sup>22</sup> However, in micelles with a crystalline core, the presence of chain folding might be expected to complicate any relationship between degree of polymerization of the core-forming block and core diameter. To investigate the potential of this prospective method of controlling core size, we first prepared two PFDMS-*b*-PI diblock copolymers with very different lengths for the core- and corona-forming blocks, namely, PFDMS<sub>133</sub>-*b*-PI<sub>1250</sub> and PFDMS<sub>21</sub>-*b*-PI<sub>132</sub> (the subscripts refer to the number-average degree of polymerization). Fiberlike micelles were prepared by dissolution of the diblock copolymers in hexane, which is a selective solvent for the PI block, followed by sonication and self-seeding at 70 °C (see the Supporting Information for details).<sup>17c,d</sup> After dissolution in a selective solvent, PFDMS block copolymers with a long PFDMS core-forming block (e.g., PFDMS<sub>133</sub>-*b*-PI<sub>1250</sub>) initially form a mixture of spherical micelles (with amorphous cores) and fiberlike micelles. The transition from spheres to fibers at ambient temperature usually requires a substantial period of time to complete (normally over a week) due to slow core crystallization.<sup>23</sup> However, self-seeding at a higher temperature effectively accelerates this transition.

As shown by transmission electron microscopy (TEM) images which reveal the electron dense Fe-containing core (Figure 1a,d), the PFDMS<sub>133</sub>-*b*-PI<sub>1250</sub> fiberlike micelles (core width,  $W_{\text{core}} = \sim 23$  nm) possessed a significantly thicker core than those for the PFDMS<sub>21</sub>-*b*-PI<sub>132</sub> micelles ( $W_{\text{core}} = \sim 8$  nm) (Scheme S1). Atomic force microscopy (AFM) analysis (Figure 1b,c,e,f) showed that the height of the PFDMS<sub>133</sub>-*b*-PI<sub>1250</sub> micelles ( $H_{\text{micelle}} = \sim 9.5$  nm) was also larger than that for the PFDMS<sub>21</sub>-*b*-PI<sub>132</sub> fibers ( $H_{\text{micelle}} = \sim 7$  nm). As the  $H_{\text{micelle}}$  values include a contribution from the corona, they provide an

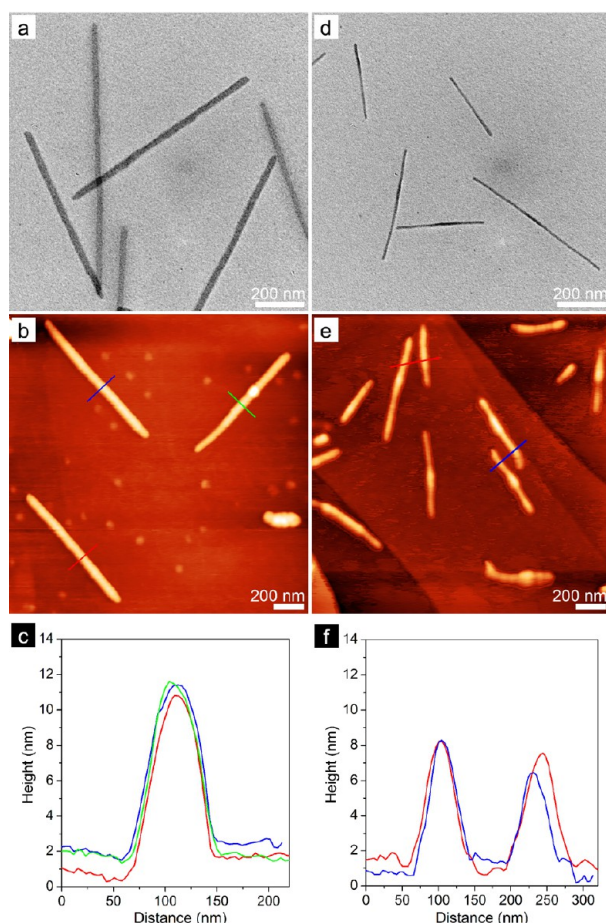


**Figure 1.** TEM images, AFM height images, and height profiles of fiberlike micelles formed by (a–c) PFDMs<sub>133</sub>-*b*-PI<sub>1250</sub> and (d–f) PFDMs<sub>21</sub>-*b*-PI<sub>132</sub> in hexane.

upper limit for the height of the core. However, based on the observation that the micelle width is much larger than the height by AFM, the low  $T_g$  PI corona appears to spread out on the substrate and so the coronal contribution to the measured value of  $H_{\text{micelle}}$  is expected to be relatively small.

The TEM and AFM data clearly suggest that the cores of the PFDMs<sub>133</sub>-*b*-PI<sub>1250</sub> micelles possess either an elliptical or rectangular cross-section based on the smaller value for the height than the width (9.5 nm (AFM) vs 23 nm (TEM)). To probe this interesting issue further, TEM images of slices microtomed from solid samples of micelles dried from the hexane solutions were obtained (Figure 2; see the Supporting Information for experimental details).<sup>24</sup> The PFDMs<sub>133</sub>-*b*-PI<sub>1250</sub> micelles showed a highly elliptical and almost rectangular cross-section for the core with the height  $H_{\text{core}} = \sim 8$  nm and width  $W_{\text{core}} = \sim 20$  nm (Figure 2a,c), which were in accordance with the values determined by AFM and by TEM, respectively. On the other hand, the cores of the PFDMs<sub>21</sub>-*b*-PI<sub>132</sub> micelles exhibited a more circular and apparently only slightly elliptical cross-section with a diameter of  $\sim 7$  nm (Figure 2b,d), which is similar to the values for  $W_{\text{core}} = \sim 8$  nm from TEM analysis of individual isolated micelles (Figure 1d) and  $H_{\text{core}} \sim H_{\text{micelle}} = \sim 7$  nm by AFM.

(b). *PFDMs-b-P2VP Block Copolymers.* In order to explore the generality of the approach to varying micelle core width, we also studied fiberlike micelles formed by two PFDMs-*b*-P2VP diblock copolymers with large differences in the degrees of

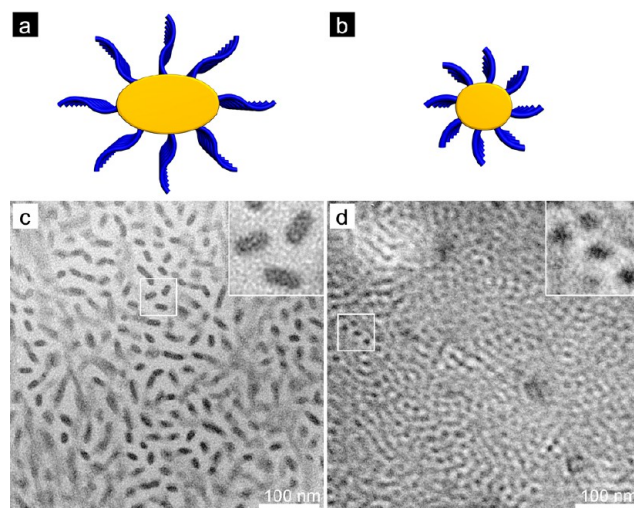


**Figure 2.** Schematic representations and TEM images of cross-sections of (a and c) PFDMs<sub>133</sub>-*b*-PI<sub>1250</sub> and (b and d) PFDMs<sub>21</sub>-*b*-PI<sub>132</sub> micelles. TEM samples were prepared by microtoming of solid samples of micelles dried from colloidal hexane solutions.

polymerization for PFDMs, namely, PFDMs<sub>48</sub>-*b*-P2VP<sub>414</sub> and PFDMs<sub>20</sub>-*b*-P2VP<sub>140</sub>.<sup>21</sup> In this case, isopropanol was used as the selective solvent for the hydrophilic P2VP corona-forming block. Similar to the case for the PFDMs-*b*-PI micelles, TEM and AFM analyses (Figure S1) revealed that the diblock copolymer with a higher degree of polymerization for PFDMs, PFDMs<sub>48</sub>-*b*-P2VP<sub>414</sub>, formed fiberlike micelles with a core of substantially greater width ( $W_{\text{core}} = \sim 20$  nm,  $H_{\text{micelle}} = \sim 23$  nm) than those formed by PFDMs<sub>20</sub>-*b*-P2VP<sub>140</sub> ( $W_{\text{core}} = \sim 7.5$  nm,  $H_{\text{micelle}} = \sim 8$  nm). Once again, the micelle width by AFM was much greater than the height, suggesting that the corona spreads out on the substrate, making the anticipated coronal contribution to  $H_{\text{micelle}}$  relatively small. Thus, in contrast to the core cross-section of PFDMs<sub>133</sub>-*b*-PI<sub>1250</sub> micelles which was found to be highly ellipsoidal or rectangular, based on the TEM and AFM data, the thicker micelles formed by PFDMs<sub>48</sub>-*b*-P2VP<sub>414</sub> possess a PFDMs core of approximately the same width and height (ca. 20 nm vs 23 nm). Although cross-sectional TEM data could not be obtained in this case, the results indicate that for these micelles the cross-section was more circular (Figure S1). The cross-sectional shape appeared to be similar for the PFDMs<sub>20</sub>-*b*-P2VP<sub>140</sub> micelles ( $W_{\text{core}} = \sim 7.5$  nm (TEM),  $H_{\text{micelle}} = \sim 8$  nm (AFM)), which appear to possess a similar cross-sectional shape to the micelles of the PI counterpart with a shorter PFDMs block, PFDMs<sub>21</sub>-*b*-PI<sub>132</sub>.

**2. Attempted Formation of Branched Micelles by Seeded Growth.** (a). *PFDMs-b-PI Block Copolymers.* The large difference in core width for the PFDMs<sub>133</sub>-*b*-PI<sub>1250</sub> and PFDMs<sub>21</sub>-*b*-PI<sub>132</sub> micelles (ca. 23 nm vs 8 nm) suggested that it might be possible to prepare branched micelles through living CDSA. With this in mind, unimers of PFDMs<sub>21</sub>-*b*-PI<sub>132</sub> in a small amount of THF (a good solvent for both blocks) were added to a solution of the PFDMs<sub>133</sub>-*b*-PI<sub>1250</sub> micelle seeds ( $L_n = 715$  nm,  $L_w/L_n = 1.06$ , where  $L_n$  and  $L_w$  are the number- and weight-average length, respectively) in hexane at room temperature (23 °C). Surprisingly, however, this gave rise to linear micelles comprising a central segment with a thicker core derived from the PFDMs<sub>133</sub>-*b*-PI<sub>1250</sub> micelle seeds and a single new segment emerging from each seed terminus with a thinner core derived from the added PFDMs<sub>21</sub>-*b*-PI<sub>132</sub> unimers (Figure

3a). Interestingly, these micelles were found to possess a gradient junction between the central seed and the newly

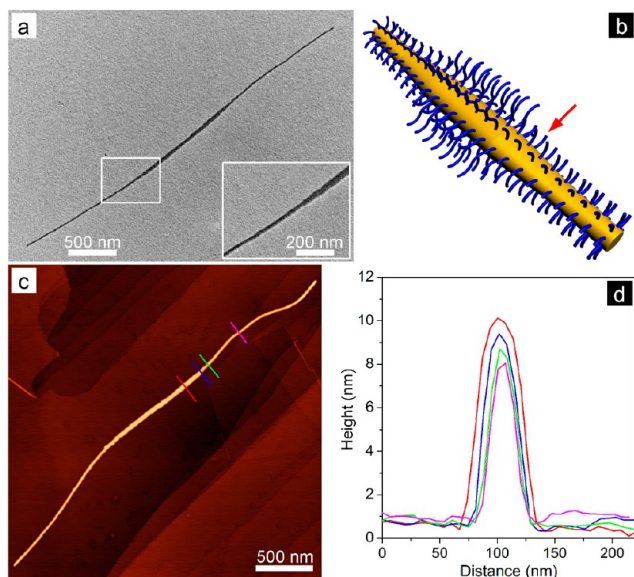


**Figure 3.** (a) TEM images, (b) schematic representation, (c) AFM height image, and (d) height profiles of linear “javelin-like” micelles formed by the addition of PFDMS<sub>21</sub>-*b*-PI<sub>132</sub> unimers in a small amount of THF to a solution of PFDMS<sub>133</sub>-*b*-PI<sub>1250</sub> micelle seeds in hexane at room temperature. Red arrow in (b) indicates the gradient junction with gradually decreasing core size.

created fibers, where the core width gradually decreased from ~23 to ~8 nm, giving rise to an overall “javelin-like” morphology (Figure 3a,b). The existence of a gradient junction was also confirmed by AFM analysis, which showed a smooth decrease of both width (from ~70 to ~45 nm) and height (from ~9.5 to ~7.2 nm) (Figures 3c,d and S2).

(b). *PFDMS-*b*-P2VP Block Copolymers.* We also attempted to form branched micelles by exploiting the difference in core width between the PFDMS<sub>48</sub>-*b*-P2VP<sub>414</sub> ( $W_{\text{core}} \approx 20$  nm) and PFDMS<sub>20</sub>-*b*-P2VP<sub>140</sub> micelles ( $W_{\text{core}} \approx 7.5$  nm).<sup>21</sup> In marked contrast to the PFDMS-*b*-PI system, the solution obtained by the addition of PFDMS<sub>20</sub>-*b*-P2VP<sub>140</sub> unimers to the seed solution of PFDMS<sub>48</sub>-*b*-P2VP<sub>414</sub> micelles ( $L_n = 550$  nm,  $L_w/L_n = 1.03$ ) in isopropanol at room temperature showed the presence of predominantly (~94%) branched micelles with a thicker central segment derived from the seeds and multiple thinner branches grown at the termini by TEM and AFM (Figure 4). The core diameter of the branches (~7.5 nm) was comparable with that of the PFDMS<sub>20</sub>-*b*-P2VP<sub>140</sub> micelles prepared by self-seeding (PFDMS-*b*-P2VP Block Copolymers subsection, see above, Figure S1) but was significantly smaller in height and width than that of the central seed segment (Figure 4d). The number of branches formed at each seed end was found to vary. Thus, the terminus of the PFDMS<sub>48</sub>-*b*-P2VP<sub>414</sub> seed micelles gave rise to two and three PFDMS<sub>20</sub>-*b*-P2VP<sub>140</sub> branches in most cases, although in ca. 25% of the micelle ends only a single fiber emanated (Figure S3).

**3. Effect of Solvent Polarity and Temperature on the Formation of Branched Micelles.** (a). *PFDMS-*b*-PI Block Copolymers.* Intrigued by the strikingly different results for the PFDMS-*b*-PI and PFDMS-*b*-P2VP systems, we performed an additional investigation on the growth by living CDSA from the ends of the large diameter seeds under different self-assembly

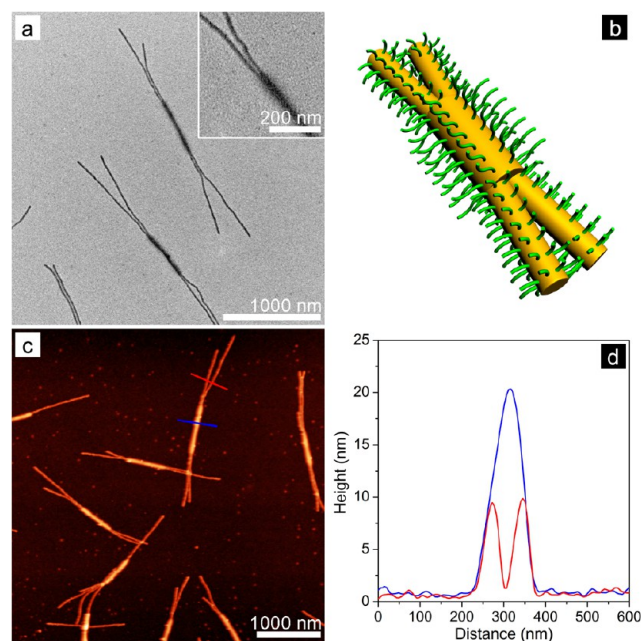


**Figure 4.** (a) TEM images, (b) schematic representation, (c) AFM height image, and (d) height profiles of branched micelles formed by the addition of PFDMS<sub>20</sub>-*b*-P2VP<sub>140</sub> unimers in a small amount of THF to a solution of PFDMS<sub>48</sub>-*b*-P2VP<sub>414</sub> micelle seeds in isopropanol at room temperature.

conditions. Bearing in mind the difference between the selective solvents hexane and isopropanol, we first considered that the polarity of solvent might play an important role in the generation of branched structures. In an initial attempt to prepare branched micelles of PFDMS-*b*-PI, we conducted the addition of unimers of PFDMS<sub>21</sub>-*b*-PI<sub>132</sub> to large diameter seed micelles of PFDMS<sub>133</sub>-*b*-PI<sub>1250</sub> in a mixture of hexane and either isopropanol or butanol to increase the polarity of the solution. However, at a volume percent of isopropanol or *n*-butanol below 40%, no branched micelles were detected, and at 40% the formation of large aggregates of micelles was observed (Figure S4). This is likely a consequence of the very poor solubility of the PI coronas in the presence of alcohols, although seeded growth appeared to occur to some extent (Figure S4).

Next, we investigated the influence of temperature, another key parameter for the crystallization of block copolymers.<sup>16,17c,d</sup> Instead of using room temperature, the addition of PFDMS<sub>21</sub>-*b*-PI<sub>132</sub> unimers in a small amount of THF to the solution of PFDMS<sub>133</sub>-*b*-PI<sub>1250</sub> micelle seeds in hexane was performed at lower temperatures. Although inefficient living growth was detected at -78 °C and at -20 °C (Figure S5), in the latter case branched micelles were formed (Figure S5a). At 0 °C, high yields (>85%) of branched micelles (Figures 5 and S6) were detected. These possessed two branches at each seed terminus in most cases (ca. 70%) and the branches exhibited a narrow length distribution (Figures 5 and S6c). Higher magnification TEM images of the branch sites (Figure 5c) indicate they are similar to those found for branched micelles derived from PFDMS-*b*-P2VP at 23 °C (Figure 4). Significantly, in contrast to the linear micelles formed by the PFDMS-*b*-PI system at room temperature (Figure 3), the micelle ends with only a single micelle emanating from the seed formed at 0 °C appeared to exhibit less of a smooth gradient and more of a step change in width (Figures 5e,f and S6a,b).

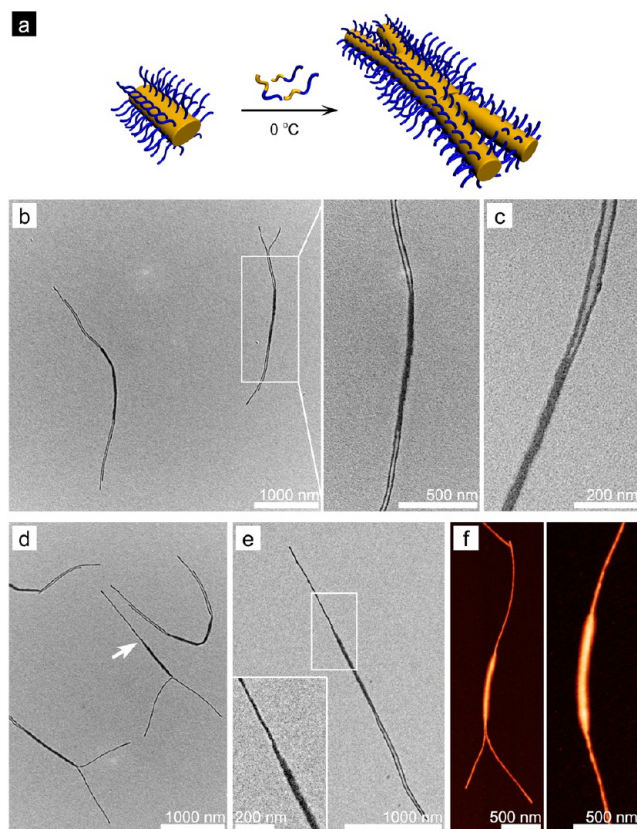


**Figure 5.** (a) Schematic representation of procedure for the formation of branched micelles of PFDMS-*b*-PI in hexane. (b and c) TEM images of branched micelles formed by the addition of PFDMS<sub>21</sub>-*b*-PI<sub>132</sub> unimers in a small amount of THF to a solution of PFDMS<sub>133</sub>-*b*-PI<sub>1250</sub> micelle seeds in hexane at 0 °C. (d–f) TEM and AFM height images showing the coexistence of micelle ends with only a single PFDMS<sub>21</sub>-*b*-PI<sub>132</sub> micelle emanating from the seed micelle terminus.

(b). *PFDMS-*b*-P2VP Block Copolymers.* We found that the micelles formed by PFDMS-*b*-P2VP were readily dispersible in a variety of alcohols with variable alkyl chain length. This allowed a facile evaluation of the effect of solvent polarity on the formation of branched micelles. Consequently, we performed the living CDSA experiments at room temperature using the PFDMS<sub>48</sub>-*b*-P2VP<sub>414</sub> micelles as seeds and PFDMS<sub>20</sub>-*b*-P2VP<sub>140</sub> as added unimers, but with ethanol (a more polar solvent than isopropanol) and *n*-butanol (a less polar solvent) as the majority component (90% in volume). For the ethanol-dominated system, the solution also yielded predominantly (ca. 81%) branched micelles as previously found in isopropanol (Figures 6a,c and S7). However, in the case of *n*-butanol, the solution produced solely linear micelles (Figure 6b,d–f), suggesting that a less polar solvent may inhibit the generation of branched structures. As shown by the high-magnification TEM image (Figure 6d, inset) and AFM analysis (Figure 6e,f), unlike the linear “javelin-like” micelles formed by the PFDMS-*b*-PI system at room temperature (Figure 3), these linear micelles possessed a step change rather than a gradient change in diameter at the interface between the thicker PFDMS<sub>48</sub>-*b*-P2VP<sub>414</sub> seeds and newly grown thinner PFDMS<sub>20</sub>-*b*-P2VP<sub>140</sub> fibers (Figure 6b).

To obtain further insight into the effect of temperature, next, we repeated the living CDSA experiments with the PFDMS-*b*-P2VP system at various temperatures. In a typical procedure for

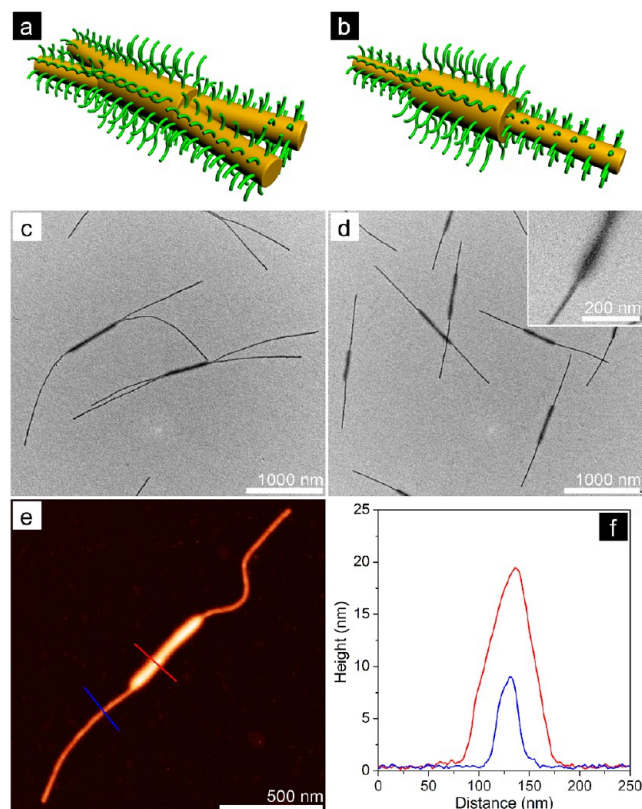


**Figure 6.** (a) Schematic representation and (c) TEM image of branched micelles formed by the addition of PFDMS<sub>20</sub>-*b*-P2VP<sub>140</sub> unimers in a small amount of THF to a solution of PFDMS<sub>48</sub>-*b*-P2VP<sub>414</sub> micelle seeds in a mixture of ethanol and isopropanol (9:1, v/v) at room temperature. (b) Schematic representation, (d) TEM images, (e) AFM height image, and (f) height profiles of linear micelles formed by the same process in a mixture of *n*-butanol and isopropanol (9:1, v/v) at room temperature.

studies at elevated temperatures, the solution of the PFDMS<sub>48</sub>-*b*-P2VP<sub>414</sub> micelle seeds in isopropanol or in a 9:1 ethanol/isopropanol mixture was heated to 45 or 60 °C and PFDMS<sub>20</sub>-*b*-P2VP<sub>140</sub> unimers in a small amount of THF were then added. The solution was allowed to age at the elevated temperature for 2 h and was then cooled to room temperature. As shown in Figures 7 and S8, the yield of branched micelles (ca. 50% for samples formed in isopropanol and ca. 35% in the case of 9:1 ethanol/isopropanol mixture) and the degree of branching dramatically decreased as the temperature was increased to 45 °C. At 60 °C, a fairly low percent of branched structures (ca. 30%) was formed in isopropanol and virtually no branching (<2%) was detected for the ethanol-dominated solution.

Similar to the case of a less polar solvent, a higher temperature also appeared to disfavor the formation of branched micelles for the PFDMS-*b*-P2VP system. Thus, rather than forming only linear micellar structures, when the aforementioned seeded growth experiment in a mixture of *n*-butanol and isopropanol (9:1, v/v) was performed at 0 °C, the generation of ca. 20% of branched micelles (Figure S9) was detected. The observation of a higher percent of branched micelles at lower temperature is in accordance with the results for the PFDMS-*b*-PI system in hexane.

**4. Versatility of the Living CDSA Route to Form Branched Block Comicelles.** The formation of branched micelles with either nonpolar (PI) or polar (P2VP) coronas in

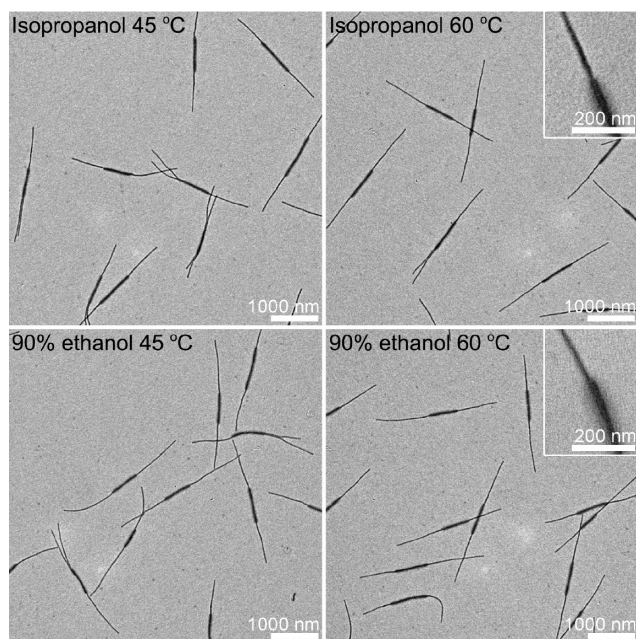
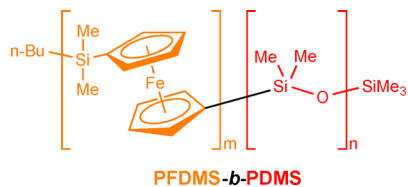


**Figure 7.** TEM images of branched and linear micelles formed by the addition of PFDMS<sub>20</sub>-*b*-P2VP<sub>140</sub> unimers in THF to solutions of PFDMS<sub>48</sub>-*b*-P2VP<sub>414</sub> micelle seeds in isopropanol and in a mixture of ethanol and isopropanol (9:1, v/v) at elevated temperatures.

various solvents suggested the existence of a general route to branched micellar structures via living CDSA involving thicker core seeds derived from PFDMS block copolymers with a longer PFDMS core-forming block and unimers with a shorter PFDMS block. In principle, the corona chemistry of both the central segment and the branches can be flexibly tailored to fit the demands of targeted applications.

To further explore the versatility of this approach, we introduced another block copolymer with a long PFDMS core-forming block and a nonpolar polydimethylsiloxane (PDMS) corona-forming block, namely, PFDMS<sub>132</sub>-*b*-PDMS<sub>1364</sub> (Chart 2). Relatively monodisperse short micelles ( $L_n = 120$  nm,  $L_w/L_n = 1.04$ ,

#### Chart 2. Structure of PFDMS-*b*-PDMS Diblock Copolymer



$L_n = 1.04$ , Figures 8a and S10) with even more highly elliptical, and perhaps more accurately almost rectangular cores ( $W_{\text{core}} = \sim 35$  nm (TEM),  $H_{\text{micelle}} = 11.5$  nm (AFM)) were prepared in decane by self-seeding at 100 °C. Compared to that for the analogue with a PI corona (see the PFDMS-*b*-PI Block Copolymers subsection 1. (a) above), such a higher temperature was used to further facilitate the transition from spherical micelles to fiberlike micelles (the transition was found to be much less efficient at 70 °C, the temperature used for PFDMS<sub>133</sub>-*b*-PI<sub>1250</sub>).

In an attempt to prepare branched micelles, unimers of PFDMS<sub>21</sub>-*b*-PI<sub>132</sub> in a small amount of THF were added to a dilute solution (in 1:9 v/v decane/hexane) of the PFDMS<sub>132</sub>-*b*-PDMS<sub>1364</sub> micelle seeds. Unlike the above case where the

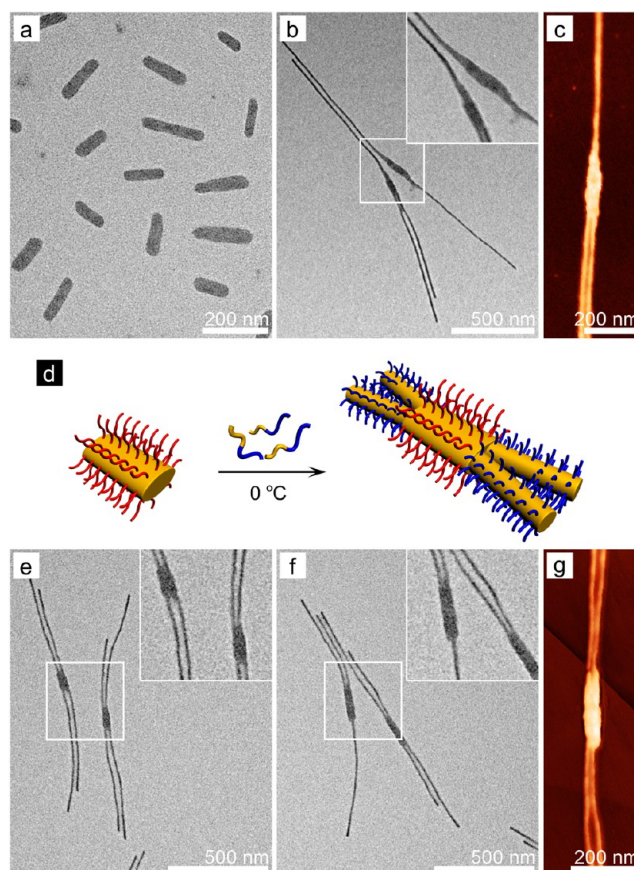


**Figure 8.** (a) TEM image of short PFDMS<sub>132</sub>-*b*-PDMS<sub>1364</sub> micelles formed in decane after sonication and self-seeding. (b) TEM and (c) AFM height images of linear and branched block comicelles formed by the addition of PFDMS<sub>21</sub>-*b*-PI<sub>132</sub> unimers in a small amount of THF to a solution of PFDMS<sub>132</sub>-*b*-PDMS<sub>1364</sub> micelle seeds in a mixture of decane and hexane (1:9, v/v) at room temperature. (d) Schematic representation of procedure for the formation of branched comicelles with a PDMS corona for the central segment and PI coronas for the branches. (e–g) TEM and AFM height images of branched block comicelles formed at 0 °C.

PFDMS<sub>133</sub>-*b*-PI<sub>1250</sub> micelles were used as seeds, the formation of branched structures was more facile in this system and a considerable amount ( $\sim 50\%$ ) of branched micelles were obtained, even at room temperature (Figures 8b,c, S11a–e, and S12a). This is likely a consequence of the larger core width of the seeds. Similar to the linear “javelin-like” micelles formed by the PFDMS-*b*-PI system at room temperature, the linear and Y-shaped micelles presented a gradient junction between the central and newly grown end segments when only a single fiber emanated from the seed terminus (Figures 8b, inset; 8c; and S11b–e). The experiment carried out at 0 °C gave rise to a much higher yield (>98%) of branched micelles with mainly two branches emanating at each seed terminus (Figures 8d–g, S11f–h, and S12b). Due to the combination of two different PFDMS block copolymers, the branched micelles actually possessed spatially segregated coronas, namely, PDMS for the central segment and PI for the branches (Figure 8d). In contrast to the analogous micelles formed at room temperature, the linear and Y-shaped micelles with a single emanating PFDMS<sub>21</sub>-*b*-PI<sub>132</sub> fiber showed a step change rather than a smooth gradient change in diameter at the junction (Figures 8f, inset and S11g,h).

We also explored the living growth of the PFDMS<sub>20</sub>-*b*-P2VP<sub>140</sub> unimers at the termini of the PFDMS<sub>132</sub>-*b*-PDMS<sub>1364</sub> micelle seeds to form amphiphilic structures containing a seed micelle with a hydrophobic periphery and branches with polar coronas (Figure 9a). A mixture of decane, hexane, and

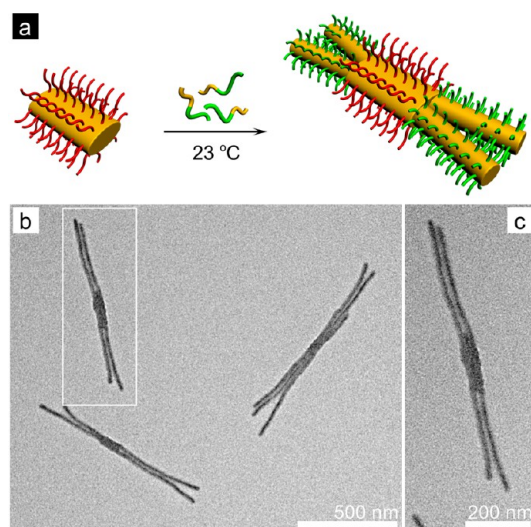


**Figure 9.** (a) Schematic representation of procedure for the formation of branched amphiphilic block comicelles with a PDMS corona for the central segment and P2VP coronas for the branches. (b and c) TEM images of branched amphiphilic block comicelles formed by the addition of PFDMS<sub>20</sub>-*b*-P2VP<sub>140</sub> unimers in a small amount of THF to a solution of PFDMS<sub>132</sub>-*b*-PDMS<sub>1364</sub> micelle seeds in a mixture of decane, hexane, and isopropanol (1:9:30, v/v/v) at room temperature.

isopropanol (1:9:30, v/v/v) was used as the solvent to overcome the solubility issues created by the presence of nonpolar and polar coronas.<sup>18d,e</sup> The living CDSA was carried out at room temperature based on the predominant existence of polar solvent. The solution eventually yielded over 98% of branched amphiphilic block comicelles with mainly 2–3 branches at each terminus and opposite corona polarities for the central segment and the branches (Figures 9 and S13). In addition, ca. 20% of branched micelles with higher number of branches (between 5 and 8 per micelle) were also detected in the solution, and it appeared that the number of branches increased for the PFDMS<sub>132</sub>-*b*-PDMS<sub>1364</sub> seed micelles due to the larger core width (~35 nm) (Figure S13). This situation seems to resemble the formation of scarf structures by seeded growth of fibers from platelet initiators.<sup>18b</sup> The formation of branched amphiphilic block comicelles was also possible when unimers of PFDMS<sub>34</sub>-*b*-P2VP<sub>272</sub> were used, but not for the case where PFDMS<sub>48</sub>-*b*-P2VP<sub>414</sub> was added (Figure S14). This indicated a threshold with respect to the PFDMS chain length of added unimers associated with the formation of branched structures.

**5. Thermal Stability of Branched Micelles.** The stability of the branched micelles was explored in a series of experiments, in which the solutions of the micelles were heated at a selected higher temperature for 2 h, and subsequently cooled slowly back to room temperature (23 °C). Generally, the branched structures were found to be retained at relative lower annealing temperatures, <~55 °C for the branched micelles formed by PFDMS<sub>133</sub>-*b*-PI<sub>1250</sub> or PFDMS<sub>132</sub>-*b*-PDMS<sub>1364</sub> with PFDMS<sub>21</sub>-*b*-PI<sub>132</sub> in hexane or in a decane/hexane mixture, and <~65 °C for those formed by PFDMS<sub>48</sub>-

*b*-P2VP<sub>414</sub> or PFDMS<sub>132</sub>-*b*-PDMS<sub>1364</sub> with PFDMS<sub>20</sub>-*b*-P2VP<sub>140</sub> in isopropanol or in isopropanol-dominated mixed solvents. However, at more elevated temperatures, an apparent transition of the branched micelles into linear products was observed. For example, on heating at 80 °C for 2 h, the branched micelles formed by PFDMS<sub>48</sub>-*b*-P2VP<sub>414</sub> and PFDMS<sub>20</sub>-*b*-P2VP<sub>140</sub> in isopropanol (~94% branched) (Figure 10b) showed a

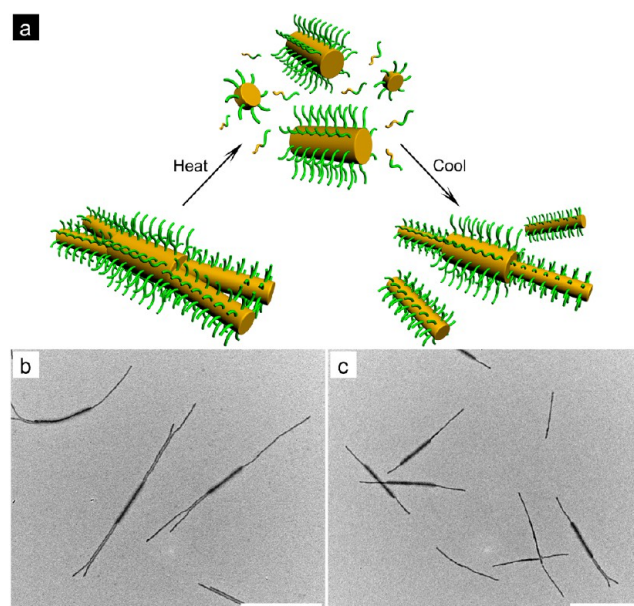


**Figure 10.** (a) Schematic representation of transformation from branched micelles to linear micelles induced by annealing at an elevated temperature. (b) TEM image of branched micelles formed by PFDMS<sub>48</sub>-*b*-P2VP<sub>414</sub> and PFDMS<sub>20</sub>-*b*-P2VP<sub>140</sub> in isopropanol before annealing. (c) TEM image of micelles obtained after heating at 80 °C for 2 h. Scale bars represent 1000 nm.

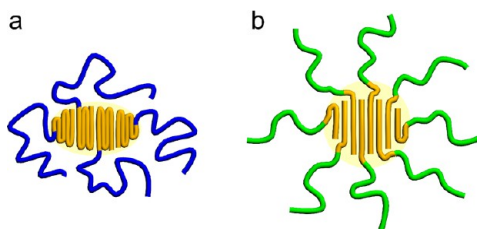
significant decrease in both the proportion of branched micelles (to ~20%) and the degree of branching (only Y-shaped branched micelles were detected, Figure 10c). The solution comprised predominantly linear block comicelles with a thicker core central segment and two thinner core end segments and homomicelles with uniform thinner cores (Figure 10a,c). Similarly, the branched micelles formed by PFDMS<sub>133</sub>-*b*-PI<sub>1250</sub> or PFDMS<sub>132</sub>-*b*-PDMS<sub>1364</sub> with PFDMS<sub>21</sub>-*b*-PI<sub>132</sub> at 0 °C also rearranged into linear “javelin-like” micelles and discrete thinner-core micelles of variable length after heating at elevated temperatures (Figure S15a,b). In contrast, the “javelin-like” micelles formed by PFDMS<sub>133</sub>-*b*-PI<sub>1250</sub> and PFDMS<sub>21</sub>-*b*-PI<sub>132</sub> at room temperature (23 °C) retained the gradient junctions after heating at 60 °C for 2 h (Figure S15c).

## DISCUSSION

**(a). Chain Folding of the PFDMS Block in the Crystalline Micelle Cores.** Given that the average distance between two adjacent ferrocenyldimethylsilane units in the PFDMS chain is ~0.65 nm,<sup>25</sup> the extended chain length of the PFDMS block ( $L_{\text{PFDMS}}$ ) would be ~86.5, ~85.8, and ~13.7 nm for PFDMS<sub>133</sub>-*b*-PI<sub>1250</sub>, PFDMS<sub>132</sub>-*b*-PDMS<sub>1364</sub>, and PFDMS<sub>21</sub>-*b*-PI<sub>132</sub>, and ~31.2 and ~13.0 nm for PFDMS<sub>48</sub>-*b*-P2VP<sub>414</sub> and PFDMS<sub>20</sub>-*b*-P2VP<sub>140</sub>, respectively. Previous synchrotron X-ray diffraction studies of the cores of electric field-aligned fiberlike PFDMS-*b*-PI micelles indicated that the chains are oriented perpendicular to fiber direction.<sup>25</sup> For micelles with a core of

elliptical or rectangular cross-section, it is expected that the PFDMS chains adopt a chain-folded orientation parallel to the short axis (see Scheme 2a for the elliptical case). The

**Scheme 2. Chain Folding of PFDMS in Cores of (a) PFDMS<sub>133</sub>-*b*-PI<sub>1250</sub> and (b) PFDMS<sub>48</sub>-*b*-P2VP<sub>414</sub> Micelles**



alternative orientation would result in a large lateral surface with a low corona chain density which would be strongly energetically disfavored on exposure to poor solvent for the core-forming block. The average number of folds of the PFDMS chains in the core can therefore be estimated by dividing  $L_{\text{PFDMS}}$  by the periodic folding length, which would approximate to  $H_{\text{core}}$ .

As summarized in Table 1, the PFDMS chains appear to be folded more than 10 times in the cores of the PFDMS<sub>133</sub>-*b*-PI<sub>1250</sub> micelles and more than 7 times for PFDMS<sub>132</sub>-*b*-PDMS<sub>1364</sub> (Scheme 2a). In contrast, for PFDMS<sub>21</sub>-*b*-PI<sub>132</sub> the number of folds was only ca. 2. It should be noted that the cross-sections of the PFDMS<sub>133</sub>-*b*-PI<sub>1250</sub> and PFDMS<sub>21</sub>-*b*-PI<sub>132</sub> micelles were of similar height ( $H_{\text{core}} \approx 8$  vs 7.0 nm, Table 1), indicating a similar folding length. The larger value for width for the PFDMS<sub>133</sub>-*b*-PI<sub>1250</sub> and PFDMS<sub>132</sub>-*b*-PDMS<sub>1364</sub> micelles is presumably the result of a higher number of chain folds (Scheme 2a). Interestingly, in the case of PFDMS-*b*-P2VP, the PFDMS chains were hardly folded in the cores (Scheme 2b), even for PFDMS<sub>48</sub>-*b*-P2VP<sub>414</sub>, where the core width approached  $\sim 20$  nm.

**(b). Kinetic versus Thermodynamic Control.** Several previous reports have indicated that crystalline lattice matching and compatible crystallization kinetics<sup>18b,20,26</sup> are required for a successful epitaxial growth in living CDSA. However, in this work, our observations of the competitive formation of branched and linear micelles and our findings that the process is modulated by subtle changes of solvent and temperature potentially offers further interesting insight into the living CDSA process. It therefore appeared important to attempt to delineate how the solvent and temperature variables are likely to affect the outcome when block copolymer unimers with a short PFDMS block are added to large diameter seeds formed from a block copolymer with a longer PFDMS block.

In a more polar solvent, that is, a very poor solvent for PFDMS, and/or at a lower temperature, the PFDMS block present in the added block copolymer unimers would be expected to rapidly deposit and crystallize when encountering a crystalline core–solvent interface associated with a seed terminus. This would be anticipated to lead to epitaxial crystallization at an initially random position on the face of the seed terminus. Moreover, the rapid deposition/crystallization process would be expected to be accompanied by substantial chain folding. This would give rise to a single fiber of narrower width emanating from the seed terminus with a location governed by the initial, random deposition. Thus, if the initial location occurred near the center of the seed terminus, the formation of linear structures with a step decrease in diameter would be expected. However, if the initial deposition is offset from the center of the seed terminus, this should leave sufficient space to facilitate the formation of branched structures (Figure 11a,b). Such branched micelles might be expected to be less stable than the corresponding linear micelles as a result of intermicelle coronal steric repulsions in the vicinity of the seed terminus. This explanation therefore suggests that the branched micelles should be considered as a kinetically trapped morphology, induced by rapid unimer deposition far from equilibrium.<sup>27</sup>

In contrast, in an only moderately poor solvent for PFDMS and/or at a higher temperature, the PFDMS block would be expected to be deposited more slowly. Thus, rather than being rapidly and randomly deposited on the seed terminus as in very poor solvents for PFDMS and/or at low temperatures, the shorter PFDMS chains would be expected to undergo a deposition process that is more thermodynamically preferred (Figure 11c,d). Thus, deposition that involves less chain folding and is dictated by the dimensions of the core–solvent interface at the seed terminus might be anticipated (Figure 11c). Subsequent epitaxial crystallization of additional unimers would be expected to give rise to the linear micellar structures in which the dimensions of the fiber emanating from the seed core are initially similar. However, it would be expected that, as the emanating fiber grows, the diameter should gradually revert to that preferred for the micelles formed by the block copolymer with shorter PFDMS chains in self-seeding experiments (for PFDMS-*b*-PI Block Copolymers see subsection 1. (a) above). The linear micelles characterized by a gradient change in diameter therefore appear to be the result of a growth process that involves deposition of unimer under conditions that are closer to equilibrium, and represent a situation nearer to thermodynamic control.

The shape of the junction in cases where only a single fiber emanates from the thicker-core seed terminus for the

**Table 1. Extended Chain Length of PFDMS block ( $L_{\text{PFDMS}}$ ) of Block Copolymers Used in This Work, Core Width ( $W_{\text{core}}$ ), and Upper Limit for Core Height ( $H_{\text{core}}$ ) of Resulting Micelles and Number of Chain Folds of PFDMS Block in the Cores**

| polymer                                               | $L_{\text{PFDMS}}$ (nm) | $W_{\text{core}}$ (nm) | $H_{\text{core}}$ (nm)   | fold (PFDMS) <sup>d</sup> |
|-------------------------------------------------------|-------------------------|------------------------|--------------------------|---------------------------|
| PFDMS <sub>133</sub> - <i>b</i> -PI <sub>1250</sub>   | $\sim 86.5$             | $\sim 23^a, \sim 20^c$ | $\sim 9.5^b, \sim 8.0^c$ | $> 10$                    |
| PFDMS <sub>21</sub> - <i>b</i> -PI <sub>132</sub>     | $\sim 13.7$             | $\sim 8^a, \sim 7^c$   | $\sim 7^{b,c}$           | $\sim 2$                  |
| PFDMS <sub>48</sub> - <i>b</i> -P2VP <sub>414</sub>   | $\sim 31.2$             | $\sim 20^a$            | $\sim 23^b$              | $< 2$                     |
| PFDMS <sub>20</sub> - <i>b</i> -P2VP <sub>140</sub>   | $\sim 13.0$             | $\sim 7.5^a$           | $\sim 8^b$               | $\sim 2$                  |
| PFDMS <sub>132</sub> - <i>b</i> -PDMS <sub>1364</sub> | $\sim 85.8$             | $\sim 35^a$            | $\sim 11.5^b$            | $> 7$                     |

<sup>a</sup> $W_{\text{core}}$  estimated by TEM data; <sup>b</sup> $H_{\text{core}}$  from AFM data where it represents an upper limit due to a corona contribution; <sup>c</sup> $W_{\text{core}}$  or  $H_{\text{core}}$  values estimated by TEM of the cross-section; <sup>d</sup>number of chain folds was calculated from  $L_{\text{PFDMS}}/H_{\text{core}}$  where the latter was determined by AFM except for the cases where a value from cross-sectional TEM was available (see Scheme S1).



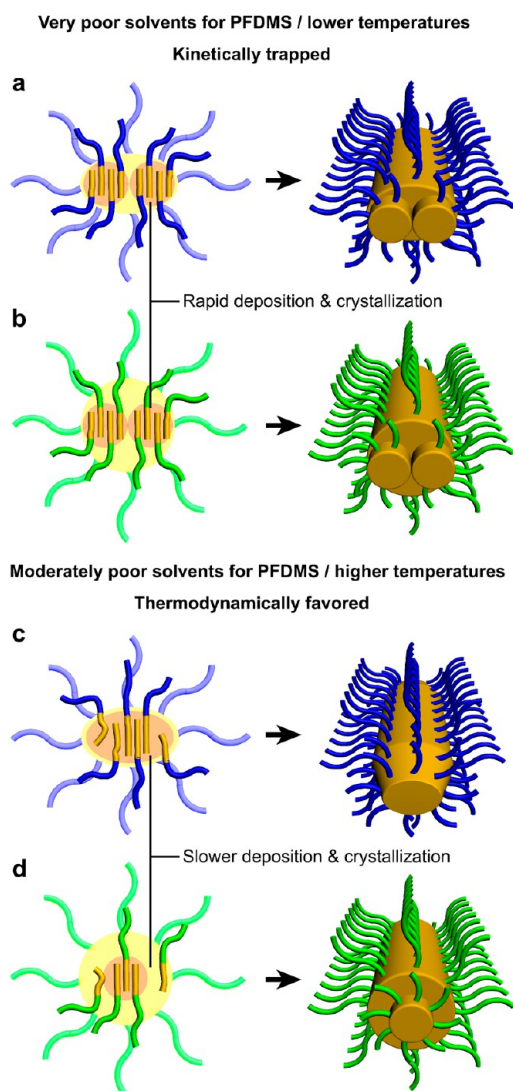


**Figure 11.** Solvent- and temperature-controlled competitive formation of branched and linear micelles (coronas: blue = PI, green = P2VP). Initial deposition and crystallization of the added unimer on the seed terminus is shown on the left, and further growth to form the emanating micelle(s) is shown on the right.

PFDMS<sub>133</sub>-*b*-PI<sub>1250</sub>/PFDMS<sub>21</sub>-*b*-PI<sub>132</sub> and PFDMS<sub>132</sub>-*b*-PDMS<sub>1364</sub>/PFDMS<sub>21</sub>-*b*-PI<sub>132</sub> systems in living CDSA experiments performed at room temperature (23 °C) were indeed characterized by such a gradient in diameter. However, in contrast, the junctions detected for any linear micelles that were formed at 0 °C (as opposed to branched structures) were characterized by a step decrease in micelle diameter (Figure 3a vs Figure 5e; Figure 8b vs f). This is presumably the result of (i) rapid deposition and epitaxial crystallization of the shorter PFDMS chains under kinetic control at lower temperatures and (ii) the existence of a slower process at higher temperatures, in which unimer deposition and crystallization proceeds under close to equilibrium conditions where the packing of the shorter PFDMS chains and the micelle diameter is initially determined by the dimensions of the core terminus.

Unlike the cases of the PFDMS-*b*-PI and PFDMS-*b*-PDMS systems, the experiments with PFDMS-*b*-P2VP consistently gave rise to junctions with a step change in radius for the linear micelles and linear components of Y-shaped branched micelles

regardless of solvent or temperature variation (Figures 4, 6, and 7). In these cases, the core cross-section appeared to be close to circular and the difference in the average core dimension between the large diameter seeds and the emanating fibers generated by the block copolymer with a shorter PFDMS block (ca. 20 nm vs 8 nm based on TEM width and AFM height data) is the largest for the materials studied (Table 1). The key factor here clearly seems to be that the shorter PFDMS core-forming block for the added unimer is unable to span the large diameter core (~20 nm) even in an extended chain conformation ( $L_{\text{PFDMS}} = 13$  nm, Table 1). This necessitates the formation of structures with a step change (Figure 11d) rather than a gradient change (Figure 11c) in diameter at the junction.

Finally, an explanation is desirable for the observation that the formation of micelles with a step change in diameter and a single emanating fiber, rather than branched structures, is preferentially found in less polar solvents, or at higher temperature in the PFDMS-*b*-P2VP system. We believe that this may reflect a thermodynamic preference for the minimization of intermicelle coronal chain repulsions at the seed terminus when deposition and crystallization occur under conditions closer to equilibrium.<sup>27</sup>

**(c). Thermal Transition from Branched Micelles to Linear micelles.** The transformation of branched micelles into linear analogs via thermal annealing (Figures 10 and S16) provided supporting evidence for the assertion that the branched structures are kinetic products while the linear micelle analogues are favored thermodynamically. During the thermal process, other types of micelles were also formed. For example, as shown in Figure S16, for the branched micelles formed by PFDMS<sub>48</sub>-*b*-P2VP<sub>414</sub> and PFDMS<sub>20</sub>-*b*-P2VP<sub>140</sub> in isopropanol, the thinner core branches were apparently less resistant to thermal treatment and dissociated into unimers and very short stublike structures at 80 °C.<sup>28</sup> However, probably due to the existence of thicker and more highly crystalline cores, the central segments derived from the seed appeared to remain intact at higher temperatures. During the cooling process, the dissolved unimers derived from PFDMS<sub>20</sub>-*b*-P2VP<sub>140</sub> appear to grow from both the thinner core stubs (yielding thinner core micelles) and also the thicker core micelles derived from the central segments. However, presumably as the growth process was initiated at a higher temperature, branched micelles are not reformed and linear structures result.

## SUMMARY

We have shown that the diameter of fiberlike micelles formed by several different crystalline-coil PFDMS block copolymers with different coronal chemistries (PI, P2VP, and PDMS) can be varied by altering the degree of polymerization of the crystallizable PFDMS core-forming block. The shapes of the cores were analyzed by TEM, cross-sectional TEM, and AFM and appear to vary from rectangular, to ellipsoidal, through to almost circular.

Using PFDMS block copolymers with different PFDMS chain lengths we have demonstrated that the growth of PFDMS block copolymer unimers with a short PFDMS core-forming block from the termini of micelle seeds with a thicker core can lead to either branched or linear structures, depending on the nature of the corona block, the quality of the solvent for PFDMS, and the temperature. The branched structures, in which 2, 3, or 4 thin fibers randomly emanate from the thicker

core terminus of the seed micelle, appear to represent a kinetically preferred morphology that results from rapid, nonequilibrium unimer deposition at the seed terminus. In contrast, the linear structures appear to represent the thermodynamically preferred morphologies.

Two different types of linear micelle structures were detected in our experiments: “javelin-type” micelles, with a gradient reduction in diameter at the junction between the seed and the emanating fiber, and linear structures with a step reduction at the seed/emanating fiber interface. “Javelin-type” micelles appear to arise from the thermodynamic preference for an initial control of the diameter of the emanating fiber by the dimensions of the seed terminus that occurs when unimer deposition and crystallization proceed under near equilibrium conditions. In contrast, a step change in diameter at the junction is favored when there is a large difference in the preferred diameter between the block copolymers used for the seed and added unimers, which makes initial dimension matching impossible. Under these circumstances, a linear micellar structure with a step-change in diameter is favored under conditions of thermodynamic control. We postulate that this preference over branched structures is a result of the lower degree of intermicelle repulsions near the junction. Interestingly, it also appears that linear micelles with a step change in diameter at the junction can also arise under conditions of kinetic control for systems where the formation of gradient junctions is possible, in which case they are mixed with branched micelles.

We have also demonstrated that using the insight gathered in this study branched micelles can be prepared from PFDMS block copolymers with diverse corona chemistries, allowing access to nonpolar, polar, and amphiphilic nanostructures. Future work will focus on studies of these morphologically interesting micelles and their applications. We are also pursuing investigations aimed at gaining further fundamental knowledge about the factors that determine the structure and cross-sectional shape of micelles with a crystalline core.

## ■ ASSOCIATED CONTENT

### Supporting Information

Experimental details and additional results. This material is available free of charge via the Internet at <http://pubs.acs.org>.

## ■ AUTHOR INFORMATION

### Corresponding Authors

ian.manners@bristol.ac.uk  
m.winnik@chem.utoronto.ca

### Notes

The authors declare no competing financial interest.

## ■ ACKNOWLEDGMENTS

This work was funded by the European Research Council (ERC) (Advanced Investigator Grant to I.M.). H.Q. also acknowledges the EU for a Marie Curie Postdoctoral Fellowship, and V.A.D. thanks the Deutsche Forschungsgemeinschaft (DFG) for a Postdoctoral Fellowship. M.A.W. thanks the NSERC of Canada for financial support. The authors thank the Electron Microscopy Unit (School of Chemistry, University of Bristol) for support on TEM and AFM imaging. The authors also thank Dr. Gerald Guerin (Department of Chemistry, University of Toronto) and Dr.

George Whittell (School of Chemistry, University of Bristol) for helpful discussions.

## ■ REFERENCES

- (1) (a) Manna, L.; Milliron, D. J.; Meisel, A.; Scher, E. C.; Alivisatos, A. P. *Nat. Mater.* **2003**, *2*, 382–385. (b) Jun, Y.-W.; Choi, J.-S.; Cheon, J. *Angew. Chem., Int. Ed.* **2006**, *45*, 3414–3439. (c) Deka, S.; Miszta, K.; Dorfs, D.; Genovese, A.; Bertoni, G.; Manna, L. *Nano Lett.* **2010**, *10*, 3770–3776. (d) Chen, S.; Wang, Z. L.; Ballato, J.; Foulger, S. H.; Carroll, D. L. *J. Am. Chem. Soc.* **2003**, *125*, 16186–16187. (e) Grebinski, J. W.; Hull, K. L.; Zhang, J.; Kosel, T. H.; Kuno, M. *Chem. Mater.* **2004**, *16*, 5260–5272. (f) Zitoun, D.; Pinna, N.; Frolet, N.; Belin, C. *J. Am. Chem. Soc.* **2005**, *127*, 15034–15035.
- (2) Milliron, D. J.; Hughes, S. M.; Cui, Y.; Manna, L.; Li, J.; Wang, L.-W.; Alivisatos, A. P. *Nature* **2004**, *430*, 190–195.
- (3) Dick, K. A.; Deppert, K.; Larsson, M. W.; Mårtensson, T.; Seifert, W.; Wallenberg, L. R.; Samuelson, L. *Nat. Mater.* **2004**, *3*, 380–384.
- (4) Miszta, K.; de Graaf, J.; Bertoni, G.; Dorfs, D.; Brescia, R.; Marras, S.; Ceseracciu, L.; Cingolani, R.; van Roij, R.; Dijkstra, M.; Manna, L. *Nat. Mater.* **2011**, *10*, 872–876.
- (5) (a) Danion, D.; Talmon, Y.; Levy, H.; Beinert, G.; Zana, R. *Science* **1995**, *269*, 1420–1421. (b) Lin, Z. *Langmuir* **1996**, *12*, 1729–1737. (c) Cardiel, J. J.; Dohnalkova, A. C.; Dubash, N.; Zhao, Y.; Cheung, P.; Shen, A. Q. *Proc. Natl. Acad. Sci. U. S. A.* **2013**, *110*, E1653–E1660. (d) Tlusty, T.; Safran, S. A. *Science* **2000**, *290*, 1328–1331. (e) Tang, M.; Carter, W. C. *J. Phys. Chem. B* **2013**, *117*, 2898–2905.
- (6) (a) Jain, S.; Bates, F. S. *Science* **2003**, *300*, 460–464. (b) Jain, S.; Bates, F. S. *Macromolecules* **2004**, *37*, 1511–1523. (c) Geng, Y.; Ahmed, F.; Bhasin, N.; Discher, D. E. *J. Phys. Chem. B* **2005**, *109*, 3772–3779. (d) Walther, A.; Goldmann, A. S.; Yelamanchili, R. S.; Drechsler, M.; Schmalz, H.; Eisenberg, A.; Müller, A. H. E. *Macromolecules* **2008**, *41*, 3254–3260. (e) Zhang, M.; Wang, M.; He, S.; Qian, J.; Saffari, A.; Lee, A.; Kumar, S.; Hassan, Y.; Guenther, A.; Scholes, G.; Winnik, M. A. *Macromolecules* **2010**, *43*, 5066–5074.
- (7) Alexandridis, P.; Lindman, B. *Amphiphilic Block Copolymers: Self-Assembly and Applications*; Elsevier Science B. V.: Amsterdam, 2000.
- (8) (a) Cameron, N. S.; Corbierre, M. K.; Eisenberg, A. *Can. J. Chem.* **1999**, *77*, 1311–1326. (b) Lodge, T. P. *Macromol. Chem. Phys.* **2003**, *204*, 265–273. (c) Mai, Y.; Eisenberg, A. *Chem. Soc. Rev.* **2012**, *41*, 5969–5985. (d) Schacher, F. H.; Rupar, P. A.; Manners, I. *Angew. Chem., Int. Ed.* **2012**, *51*, 7898–7921. (e) Blanazs, A.; Armes, S. P.; Ryan, A. J. *Macromol. Rapid Commun.* **2009**, *30*, 267–277.
- (9) Hayward, R. C.; Pochan, D. J. *Macromolecules* **2010**, *43*, 3577–3584.
- (10) Won, Y.-Y.; Davis, H. T.; Bates, F. S. *Macromolecules* **2003**, *36*, 953–955.
- (11) (a) Cui, H.; Chen, Z.; Zhong, S.; Wooley, K. L.; Pochan, D. J. *Science* **2007**, *317*, 647–650. (b) Li, Z.; Chen, Z.; Cui, H.; Hales, K.; Wooley, K. L.; Pochan, D. J. *Langmuir* **2007**, *23*, 4689–4694.
- (12) (a) Gröschel, A. H.; Schacher, F. H.; Schmalz, H.; Borisov, O. V.; Zhulina, E. B.; Walther, A.; Müller, A. H. E. *Nat. Commun.* **2012**, *3*, 710. (b) Gröschel, A. H.; Walther, A.; Löbbling, T. I.; Schacher, F. H.; Schmalz, H.; Müller, A. H. E. *Nature* **2013**, *503*, 247–251.
- (13) Dupont, J.; Liu, G.; Niihara, K.; Kimoto, R.; Jinnai, H. *Angew. Chem., Int. Ed.* **2009**, *48*, 6144–6147.
- (14) (a) Pochan, D. J.; Chen, Z.; Cui, H.; Hales, K.; Qi, K.; Wooley, K. L. *Science* **2004**, *306*, 94–97. (b) Chen, Z.; Cui, H.; Hales, K.; Li, Z.; Qi, K.; Pochan, D. J.; Wooley, K. L. *J. Am. Chem. Soc.* **2005**, *127*, 8592–8593. (c) Cui, H.; Chen, Z.; Wooley, K. L.; Pochan, D. J. *Soft Matter* **2009**, *5*, 1269–1278.
- (15) For self-assembly of PFDMS-derived crystalline-coil block copolymers: (a) Massey, J. A.; Temple, K.; Cao, L.; Rharbi, Y.; Raez, J.; Winnik, M. A.; Manners, I. *J. Am. Chem. Soc.* **2000**, *122*, 11577–11584. (b) Cao, L.; Manners, I.; Winnik, M. A. *Macromolecules* **2002**, *35*, 8258–8260.
- (16) For recent work on the self-assembly of other crystalline-coil block copolymers: (a) Zheng, J. X.; Xiong, H.; Chen, W. Y.; Lee, K.; Van Horn, R. M.; Quirk, R. P.; Lotz, B.; Thomas, E. L.; Shi, A.-C.;

Cheng, S. Z. D. *Macromolecules* **2006**, *39*, 641–650. (b) Du, Z.-X.; Xu, J.-T.; Fan, Z.-Q. *Macromolecules* **2007**, *40*, 7633–7637. (c) Lazzari, M.; Scalarone, D.; Hoppe, C. E.; Vazquez-Vazquez, C.; López-Quintela, M. A. *Chem. Mater.* **2007**, *19*, 5818–5820. (d) Schmalz, H.; Schmelz, J.; Drechsler, M.; Yuan, J.; Walther, A.; Schweimer, K.; Mihut, A. M. *Macromolecules* **2008**, *41*, 3235–3242. (e) Mihut, A. M.; Drechsler, M.; Möller, M.; Ballauff, M. *Macromol. Rapid Commun.* **2010**, *31*, 449–453. (f) Patra, S. K.; Ahmed, R.; Whittell, G. R.; Lunn, D. J.; Dunphy, E. L.; Winnik, M. A.; Manners, I. *J. Am. Chem. Soc.* **2011**, *133*, 8842–8845. (g) Petzetakis, N.; Dove, A. P.; O'Reilly, R. K. *Chem. Sci.* **2011**, *2*, 955–960. (h) Jia, L.; Lévy, D.; Durand, D.; Impéror-Clerc, M.; Cao, A.; Li, M.-H. *Soft Matter* **2011**, *7*, 7395–7403. (i) Gao, Y.; Li, X.; Hong, L.; Liu, G. *Macromolecules* **2012**, *45*, 1321–1330. (j) Schmelz, J.; Schedl, A. E.; Steinlein, C.; Manners, I.; Schmalz, H. *J. Am. Chem. Soc.* **2012**, *134*, 14217–14225. (k) Yin, L.; Lodge, T. P.; Hillmyer, M. A. *Macromolecules* **2012**, *45*, 9460–9467. (l) Lee, C.-U.; Smart, T. P.; Guo, L.; Epps, T. H., III; Zhang, D. *Macromolecules* **2011**, *44*, 9574–9585. (m) Lee, C.-U.; Lu, L.; Chen, J.; Garno, J. C.; Zhang, D. *ACS Macro Lett.* **2013**, *2*, 436–440. (n) Petzetakis, N.; Robin, M. P.; Patterson, J. P.; Kelley, E. G.; Cotanda, P.; Bomans, P. H. H.; Sommerdijk, N. A. J. M.; Dove, A. P.; Epps, T. H., III; O'Reilly, R. K. *ACS Nano* **2013**, *7*, 1120–1128. (o) Lee, I.-H.; Amaladass, P.; Yoon, K.-Y.; Shin, S.; Kim, Y.-J.; Kim, I.; Lee, E.; Choi, T.-L. *J. Am. Chem. Soc.* **2013**, *135*, 17695–17698. (p) Yu, B.; Jiang, X.; Yin, J. *Macromolecules* **2014**, *47*, 4761–4768. (q) Qian, J.; Li, X.; Lunn, D. J.; Gwyther, J.; Hudson, Z. M.; Kynaston, E.; Rupa, P. A.; Winnik, M. A.; Manners, I. *J. Am. Chem. Soc.* **2014**, *136*, 4121–4124. (r) Rizis, G.; van de Ven, T. G. M.; Eisenberg, A. *Angew. Chem., Int. Ed.* **2014**, *53*, 9000–9003. (s) Hudson, Z. M.; Boott, C. E.; Robinson, M. E.; Rupa, P. A.; Winnik, M. A.; Manners, I. *Nat. Chem.* **2014**, *6*, 893–898.

(17) (a) Wang, X.; Guerin, G.; Wang, H.; Wang, Y.; Manners, I.; Winnik, M. A. *Science* **2007**, *317*, 644–647. (b) Gilroy, J. B.; Gädt, T.; Whittell, G. R.; Chabanne, L.; Mitchels, J. M.; Richardson, R. M.; Winnik, M. A.; Manners, I. *Nat. Chem.* **2010**, *2*, 566–570. (c) Qian, J.; Guerin, G.; Lu, Y.; Cambridge, G.; Manners, I.; Winnik, M. A. *Angew. Chem., Int. Ed.* **2011**, *50*, 1622–1625. (d) Qian, J.; Lu, Y.; Chia, A.; Zhang, M.; Rupa, P. A.; Gunari, N.; Walker, G. C.; Cambridge, G.; He, F.; Guerin, G.; Manners, I.; Winnik, M. A. *ACS Nano* **2013**, *7*, 3754–3766.

(18) (a) Wang, H.; Lin, W.; Fritz, K. P.; Scholes, G. D.; Winnik, M. A.; Manners, I. *J. Am. Chem. Soc.* **2007**, *129*, 12924–12925. (b) Gädt, T.; Jeong, N. S.; Cambridge, G.; Winnik, M. A.; Manners, I. *Nat. Mater.* **2009**, *8*, 144–150. (c) Rupa, P. A.; Cambridge, G.; Winnik, M. A.; Manners, I. *J. Am. Chem. Soc.* **2011**, *133*, 16947–16957. (d) Rupa, P. A.; Chabanne, L.; Winnik, M. A.; Manners, I. *Science* **2012**, *337*, 559–562. (e) Qiu, H.; Russo, G.; Rupa, P. A.; Chabanne, L.; Winnik, M. A.; Manners, I. *Angew. Chem., Int. Ed.* **2012**, *51*, 11882–11885.

(19) (a) Kamps, A. C.; Fryd, M.; Park, S.-J. *ACS Nano* **2012**, *6*, 2844–2852. (b) Lee, E.; Hammer, B.; Kim, J.-K.; Page, Z.; Emrick, T.; Hayward, R. C. *J. Am. Chem. Soc.* **2011**, *133*, 10390–10393. (c) Kim, J.-K.; Cho, C.-H.; Paek, K.; Jo, M.; Park, M.; Lee, N.-E.; Kim, Y.; Kim, B. J.; Lee, E. *J. Am. Chem. Soc.* **2014**, *136*, 2767–2774.

(20) Qiu, H.; Cambridge, G.; Winnik, M. A.; Manners, I. *J. Am. Chem. Soc.* **2013**, *135*, 12180–12183.

(21) For a brief communication on the formation of branched micelles with PFDMS-*b*-P2VP, see: Qiu, H.; Du, V. A.; Winnik, M. A.; Manners, I. *J. Am. Chem. Soc.* **2013**, *135*, 17739–17742.

(22) Previous studies on scaling relations for various block copolymer-based spherical and fiberlike micelles that possess an amorphous core showed that the core diameter increased with an increase in the length of the core-forming block. For a few examples, see: (a) Zhang, L.; Barlow, R. J.; Eisenberg, A. *Macromolecules* **1995**, *28*, 6055–6066. (b) Zhang, L.; Eisenberg, A. *J. Am. Chem. Soc.* **1996**, *118*, 3168–3181. (c) Zheng, Y.; Won, Y.-Y.; Bates, F. S.; Davis, H. T.; Scriven, L. E.; Talmon, Y. *J. Phys. Chem. B* **1999**, *103*, 10331–10334.

(23) Hsiao, M.-S.; Yusoff, S. F. M.; Winnik, M. A.; Manners, I. *Macromolecules* **2014**, *47*, 2361–2372.

(24) Previous studies on the cross-sections of shell-crosslinked PFDMS<sub>50</sub>-*b*-PI<sub>250</sub> micelles with much shorter PFDMS core-forming

blocks by TEM also suggested an elliptical or circular cross-section for the core. See: Wang, X.; Liu, K.; Arsenault, A. C.; Rider, D. A.; Ozin, G. A.; Winnik, M. A.; Manners, I. *J. Am. Chem. Soc.* **2007**, *129*, 5630–5639.

(25) Gilroy, J. B.; Rupa, P. A.; Whittell, G. R.; Chabanne, L.; Terrill, N. J.; Winnik, M. A.; Manners, I.; Richardson, R. M. *J. Am. Chem. Soc.* **2011**, *133*, 17056–17062.

(26) Gädt, T.; Schacher, F. H.; McGrath, N.; Winnik, M. A.; Manners, I. *Macromolecules* **2011**, *44*, 3777–3786.

(27) We also considered whether contraction of the coronal chains to expose a greater area of the core at the fiber terminus under conditions of poor solvation or low temperature might explain the preference for branched rather than linear structures. However, this explanation does not agree with experimental observations. For example, we found by dynamic light scattering (DLS) that *n*-butanol is a poorer solvent for P2VP than ethanol and so the formation of branched structures would be favored in the former whereas the reverse situation is found (see Figure S17 for DLS data).

(28) Previous studies showed that long fiberlike micelles of PFDMS block copolymers are fragile and may fragment when the colloidal solutions are heated, presumably caused by shear forces associated with convection of the solvent. See: Qian, J.; Lu, Y.; Cambridge, G.; Guerin, G.; Manners, I.; Winnik, M. A. *Macromolecules* **2012**, *45*, 8363–8372.